Saturation Field of Frustrated Chain Cuprates: Broad Regions of Predominant Interchain Coupling

S. Nishimoto,[1] S.-L. Drechsler,[1,*] R. O. Kuzian,[1] J. van den Brink,[1] J. Richter,[2] W. E. A. Lorenz,[1] Y. Skourski,[3] R. Klingeler,[4] and B. Büchner[1]

[1]*IFW Dresden, P.O. Box 270116, D-01171 Dresden, Germany*
[2]*Universität Magdeburg, Institut für Theoretische Physik, Germany*
[3]*Hochfeld-Magnetlabor Dresden, Helmholtz-Zentrum Dresden-Rossendorf, D-01314 Dresden, Germany*
[4]*Kirchhoff Institute for Physics, University of Heidelberg, D-69120 Heidelberg, Germany*

(Received 19 April 2010; revised manuscript received 1 April 2011; published 22 August 2011)

A thermodynamic method to extract the interchain coupling (IC) of spatially anisotropic 2D or 3D spin-1/2 systems from their empirical saturation field H_s ($T = 0$) is proposed. Using modern theoretical methods we study how H_s is affected by an antiferromagnetic (AFM) IC between frustrated chains described in the J_1-J_2-spin model with ferromagnetic 1st and AFM 2nd neighbor in-chain exchange. A complex 3D-phase diagram has been found. For Li_2CuO_2 and $Ca_2Y_2Cu_5O_{10}$, we show that H_s is solely determined by the IC and predict $H_s \approx 61$ T for the latter. With $H_s \approx 55$ T from magnetization data one reads out a weak IC for Li_2CuO_2 close to that obtained from inelastic neutron scattering.

DOI: 10.1103/PhysRevLett.107.097201 PACS numbers: 75.10.Jm, 75.30.Cr, 75.30.Et

Since real spin chain systems exhibit besides a significant in-chain coupling also an *interchain* coupling (IC), one may ask: in which cases is this relatively weak IC still important or even crucial? From the Mermin-Wagner theorem its decisive role for the suppression of fluctuations is well-known. The IC leads to long-range order at $T = 0$ in 2D [1] and at $T < T_N$ in 3D [2]. Often one is faced with a situation that the large in-chain couplings are known with reasonable precision, e.g., from inelastic neutron scattering (INS) or susceptibility data [3], but precise values for the tiny (nevertheless important) IC are lacking. Without magnetic frustration the IC can be determined quite accurately, e.g., from T_N analyzed by Quantum Monte Carlo studies [4]. But how to extract from experimental data a small IC for frustrated systems with weakly coupled chains where these methods do not work? Here we address such a 2D or 3D problem for the case of frustrated spin-1/2 chains with ferromagnetic (FM) 1st neighbor and antiferromagnetic (AFM) 2nd neighbor exchange described by the isotropic J_1-J_2 model (IM). Nowadays it is the standard model for edge-shared chain cuprates (see, e.g., [5]). This 1D-IM attracted much interest [6–11] due to a rich phase diagram with multipolar (MP) phases derived from multimagnon bound states (MBS) in high magnetic fields [12–14]. Additional AFM degrees of freedom enhance the kinetic energy of magnons and AFM IC might disfavor multi-MBS. Hence, a precise knowledge of the magnitude of the IC is a necessary prerequisite to attack the multi-MBS problem, including a possible MBS Bose-Einstein condensation [15–18], and thus the IC is of general interest. Since Li_2CuO_2 (see Fig. 1) is one of the best studied frustrated cuprates, it is well suited to compare theory and experiment. In particular, the main in-chain and IC J's were extracted from INS data and a specific AFM IC was found crucial for preventing spiral order in the 3D ground state (GS) [3]. If the saturation field H_s would be known, the INS derived IC could be checked. But so far H_s has not been measured for Li_2CuO_2. Here we report high-field magnetization data to fill this gap. Our paper is organized as follows. We recall the 1D case and provide details of the density-matrix renormalization group (DMRG) technique involved. Then we report results for coupled chains, including a complex phase diagram and a comparison with our experimental H_s-data for Li_2CuO_2 fully explained in terms of a predominant IC.

We apply the DMRG method [19] with periodic boundary conditions (PBC) in all directions. Seemingly, this method is less favorable for $D > 1$; however, on modern workstations using highly efficient DMRG codes, spin systems with up to about $\sqrt{10} \times \sqrt{10} \times 50$ sites, i.e., 10 coupled chains of length $L \sim 50$, can be studied. Thus, by taking a proper arrangement of the chains, 3D-lattices can be simulated cf. the inset in Fig. 2. Let us describe how the block states are constructed in an $n \times L$ cluster, where n

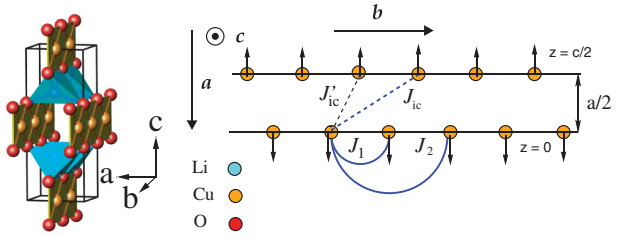

FIG. 1 (color). Left: Crystal structure of Li_2CuO_2 with two CuO_2 chains per unit cell along the b axis. Right: View along the c axis on the ab plane. The main in- and interchain couplings $J_{1,2}$ and J_{IC}, J'_{IC}: arcs and dashed lines, respectively. The normalized ICs read $\beta_1 = J'_{IC}/|J_1|$ and $\beta_2 = J_{IC}/|J_1|$.

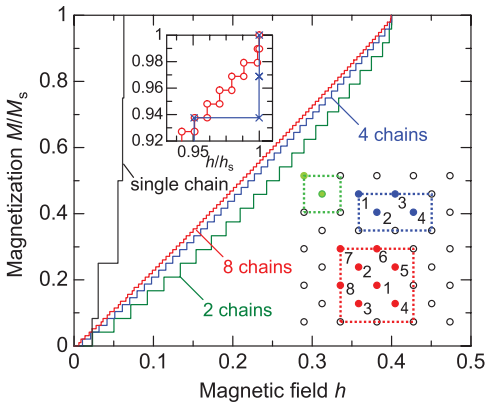

FIG. 2 (color). Magnetization vs field (DMRG data) for different n as shown in the inset, for $\alpha = J_2/|J_1| = 1/3$, $\beta_2 = 0.05$, $\beta_1 = 0$, and $L = 24$ sites in each chain. Lower inset: The 3D arrangement of chains used in our DMRG study. Upper inset: M/M_s in the 3-MBS region for $\beta_2 = 0.005$ (blue curve, ×) and the 1-magnon C phase for $\beta_2 = 0.05$ (red curve, ○). Note the 3 times larger step for $\beta_2 = 0.005$.

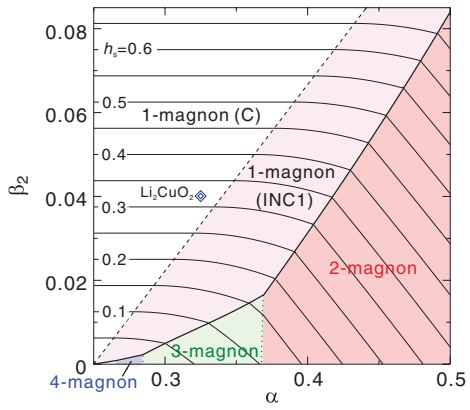

FIG. 3 (color). Part of the 3D phase diagram around Li_2CuO_2 in terms of β_2 and α. h_s is given by contour lines.

denotes the number of chains and L is the chain length. If we regard n sites in the ac-plane as a "unit cell", the system can be treated as an effective 1D chain with L sites (step 1). This enables us to use an appropriate 1D array for the construction of the PBC (see Fig. 1 of Ref. [20]). In step 2 the sites within each "unit cell" are arranged into numeric order (see the inset of Fig. 2). Thus, the distance between most separated interacting sites can be held at 11 and 23 in the 4- and 8-chain systems, respectively. Since the interactions run spatially throughout the system, the wave function converges very slowly with DMRG sweep but without getting trapped in a "false" GS. We kept $m \approx 1600$–4000 density-matrix eigenstates. About 30 sweeps are necessary to obtain the GS energy within a convergence of $10^{-7}|J_1|$ for each m value. All calculated quantities were extrapolated to $m \to \infty$ and the maximum error in the GS energy is estimated as $\Delta E/|J_1| \sim 10^{-4}$, while the discarded weight in the renormalization is less than 1×10^{-6}. For high-spin states [$S^z_{\rm tot} \geq (nL - 10)/2$)] the GS energy is obtained with an accuracy of $\Delta E/|J_1| < 10^{-12}$ by carrying out several thousands sweeps even with $m \approx 100$–800. Then, we obtain the reduced saturation field $h_s = g\mu_B H_s/|J_1|$ with high accuracy (e.g. 12 digits as compared to exact solutions available in some cases). The assignment in the 1D phase-diagrams [11–14,21] and in 3D (see Fig. 3) stems from the magnetization curves slightly below h_s (see Figs. 2 and 6). The signature of each phase is the height of the magnetization steps $\Delta S^z = 1, 2, 3, \ldots$ for di- (1-magnon), quadru- (2-MBS), octu- (3-MBS), and hexadecupolar (4-MBS), etc., phases, respectively. For the 2-MBS case the DMRG results are confirmed by the exact hard-core boson approach (HCBA) [9].

We start with the 1D problem. With $\alpha = J_2/|J_1|$, the critical point is given by a level crossing of a singlet and the highest multiplet state at $\alpha_c = 1/4$. Approaching α_c from the spiral side $\alpha \geq \alpha_c$, $H_s^{\rm 1D}(\alpha)$ decreases and vanishes at $\alpha_c \geq \alpha \geq 0$. The curve $H_s^{\rm 1D}(\alpha)$ is *not* smooth: it consists of quasilinear parts with an infinite number of slope jumps at the endpoints of each quasilinear part. These intervals become shorter and shorter when $\alpha \to \alpha_c$ (see Fig. S2 of Ref. [21]). These nonanalytic endpoints reflect the changes of multi-MBS related low-energy excitations. This specific behavior persists also in D = 2, 3 (see Figs. 4 and 5) and is a signature of quantum phase transitions. Concerning Li_2CuO_2 we stress that a 1D approach yields for $\alpha = 0.332$ [3], $h_s = 0.061\,691\,6$ (see Table I) or 10.46 T, where $g = 2$ and $J_1 = 228$ K have been used. Thus, the empirical value $H_s = 55.4$ T reported below is strongly *underestimated* by a 1D approach. Hence, let us consider, what happens, if an IC as shown in Fig. 1 is switched on. In general, a complex phase diagram in terms of the IC and α has been obtained (see Fig. 3 and Ref. [21]). First, with increasing IC above a critical $J_{\rm IC}^{\rm cr,-}(\alpha)$ the MP phase is removed in favor of one of the two incommensurate (INC) dipolar phases. Here H_s, given exactly by the spin wave theory (SWT), is still affected by both in-chain and IC although the influence of the former for $\alpha < 0.54$ is significantly reduced as compared to the 1D case (see Figs. 4 and 5). At stronger IC for $\alpha < 1$ one reaches a 2nd critical point $J_{\rm IC,2}^{\rm cr,+}$ where the INC phases are suppressed in favor of a commensurate (C) phase with FM in-chain correlations (see Figs. 3–5). Then H_s depends *solely* on the IC:

$$g\mu_B H_s = N_{\rm IC}(J_{\rm IC} + J'_{\rm IC}) \quad \text{for } J_{\rm IC} \geq J_{\rm IC}^{\rm cr,+}, \qquad (1)$$

where $N_{\rm IC}$ is the number of nearest interchain neighbors (8 for Li_2CuO_2). At $\alpha > 1$ there is no C-phase. For simplicity [22] we take $J'_{\rm IC} = 0$. Then, $J_{\rm IC}^{\rm cr,+}(\alpha)/J_1 = (1\text{–}4\alpha)/9$, if $\alpha < 0.57$ which is obeyed for Li_2CuO_2. The INC2-C transition in the interval $0.57 \leq \alpha < 1$ is of 1st order [21]. For Li_2CuO_2 [3], we have $J_{\rm IC} \approx 9$ K $> J_{\rm IC}^{\rm cr,+}(0.332) = 0.0364|J_1| \approx 8.2$ K [23]. Since in the

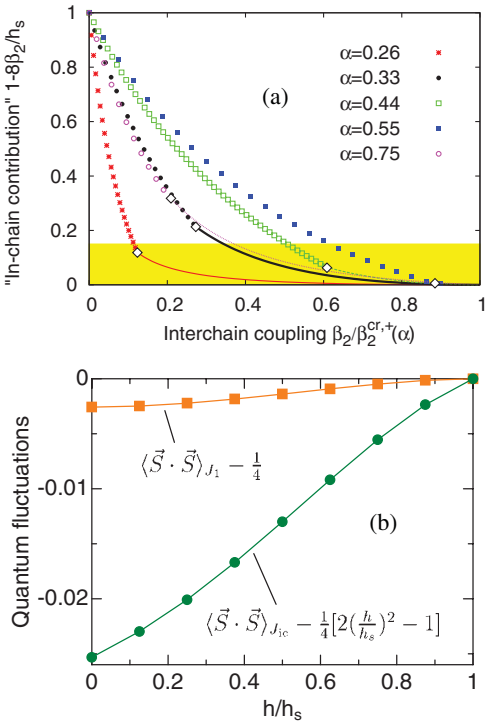

FIG. 4 (color). (a) Approximate in-chain contribution to the saturation field measured by its deviation from Eq. (1) for different α values vs β_2 in units of its critical value $\beta_2^{\mathrm{cr},+}$ (see Figs. 3, S1 of Ref. [21], and text). Yellow stripe: region of predominant IC. The full line parts of a curve (below the symbol $\diamond$) can be found within SWT, whereas the branches given by symbols are obtained by the DMRG and the HCBA. (b) in-chain and IC spin-spin correlation functions vs applied field, given by the filled symbols ■ and ●, respectively, from DMRG.

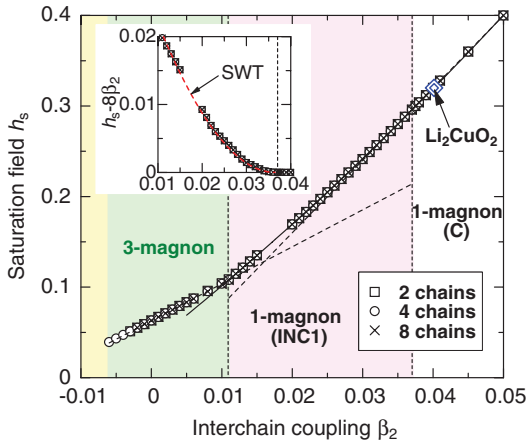

FIG. 5 (color). The saturation field h_s at $\alpha = 1/3$ vs β_2 from DMRG method. Notice the two critical IC values $\beta_2^{\mathrm{cr},-} = J_{\mathrm{IC}}^{\mathrm{cr},-}/|J_1| = 0.0109$ and $\beta_2^{\mathrm{cr},+} = J_{\mathrm{IC}}^{\mathrm{cr},+}/|J_1| = 0.037\,04$ denoted by dashed vertical lines. For INC1- and C-phases, see text. Inset: the weak nonlinearity of h_s vs β_2.

C phase H_s depends solely on J_{IC}, the IC can be read off from experiment: $H_s = 55.4$ T yielding $J_{\mathrm{IC}} = 9.25$ K very close to 9.04 K from zero-field INS data [3]. In the INC1 phase J_{IC} dominates H_s. There above $J_{\mathrm{IC}}^{\mathrm{cr},-}(0.332) \approx 0.0109|J_1| = 2.5$ K only INC 1-magnon low-energy excitations exist. Below $J_{\mathrm{IC}}^{\mathrm{cr},-}$ 3-MBS are recovered as low-energy excitations. The transition from the 3-MBS- to the INC1-phase is 1st order. The general case is shown in Fig. 4(a). Well below $J_{\mathrm{IC}}^{\mathrm{cr},+}$, H_s significantly depends on α. The yellow stripe highlights the region of predominant IC addressed in our title. Here this dependence is weak. Subtracting their classical value, the spin-spin correlation functions show that the in-chain fluctuations vanish much faster than the IC ones for $H \longrightarrow H_s$ [see Fig. 4(b)] in accord with the surprising result of Eq. (1). In the FM region $\alpha < 1/4$ the in-chain contribution vanishes by definition. Hence, the external field has to overcome the AFM IC, only, and Eq. (1) is valid. This is the case of $Ca_2Y_2Cu_5O_{10}$ [24] with an IC geometry like in Li_2CuO_2 and a 2D chain arrangement, i.e. $N_{\mathrm{IC}} = 4$. Its reduced N_{IC} is overcompensated by a larger IC $J_{\mathrm{IC}} + J'_{\mathrm{IC}} = 26$ K [25]. Then we predict $H_s \approx 61$ T refining a value of 70 T overestimated from low-field data [24].

Pulsed-field magnetization studies have been performed at the Dresden High Magnetic Field Laboratory in fields up to 60 T. The results taken at $T = 1.45$ K for $H \parallel b$ axis on a Li_2CuO_2 single crystal from the same batch as in the INS-study [3] are shown in Fig. 6. The data imply a quasi-linear increase of the magnetization $M(H)$ between 10 and 30 T, i.e. $\partial M/\partial H = M' \approx$ const. Above about 50 T M' increases notably and pronounced peaks develop at 55.4 ± 0.25 T and 55.1 ± 0.25 T for two pieces of our single crystal. The sharp drop of M' towards 0 at higher fields justifies to attribute the peaks with H_s. The saturation moment amounts to $M_s \approx 0.99 \pm 0.06\mu_{\mathrm{B}}$/f.u. using $g_b = 1.98 \pm 0.12$ in reasonable agreement with $g_b = 2.047$ from low-field ESR-data at 300 K [26]. In Fig. 6 we compare M/M_s from the DMRG with the experimental data for Li_2CuO_2. The DMRG description in this plot is

TABLE I. Saturation field h_s at $\alpha = 0.332$, $\beta_2 = 3/76$, and $\beta_1 = 0$. J_{IC} has been multiplied by 4 for 2-chain systems.

L	single chain	2-chain system	8-chain system
16	0.061 048 005 894 2	0.315 789 473 684	0.315 789 473 684
48	0.061 691 042 337 8	0.315 789 473 684	0.315 789 473 684
96	0.061 691 0487 270	0.315 789 473 684	
144	0.061 691 048 724 7	0.315 789 473 684	

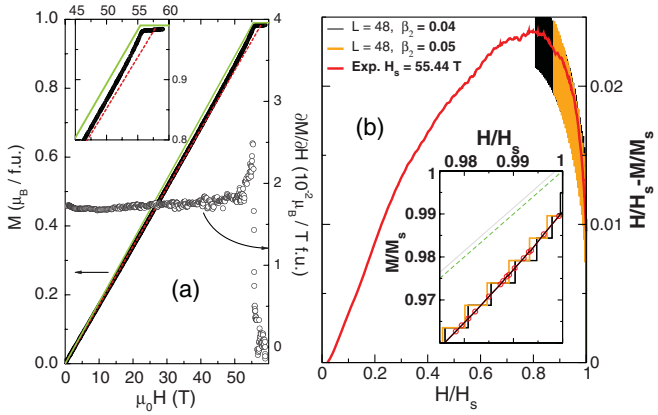

FIG. 6 (color). (a) Magnetization M (left axis) and its derivative $\partial M/\partial H$ (○) from pulsed fields. Red (green dashed) line: auxiliary line pointing out the upturn near H_s, (classical curve (CC): $M/M_s = H/H_s$). (b) Deviations from CC: DMRG vs experiment for different IC β_2 and an H_s value within the experimental error bars. Inset: Behavior just below H_s for the β_2 values of the main part.

good, but it is inconvenient to extract J's or α because of weak quantum fluctuations which hardly affect $M(H)$ for Li_2CuO_2. The function $f(M) = H/H_s - M/M_s$ reflects the quantum fluctuations much better (see Fig. 6). Notice the enhanced fluctuations (i.e. smaller $M(H)$) for the weaker IC (see inset). Noteworthy, the "width" of the DMRG curves stems from the finite steps of $M(H)$ due to the finite L. The almost straight shape of the $M(H)$ curves shown in Fig. 6 evidences the 3D character of Li_2CuO_2 in accord with the large local magnetic moment $\approx 0.93\mu_B$ observed in the ordered phase at low T at $H = 0$. The measured H_s of our single crystal yields $J_{IC} = 9.25 \pm 0.04$ K, close to the INS data mentioned above. Notably, linear relations of two experimentally accessible quantities, the Curie-Weiss temperature and H_s, yield useful constraints for J_1 and J_2 [21].

To summarize, the crucial role of AFM IC in frustrated quasi-1D systems, such as Li_2CuO_2, for their behavior in external fields and, particularly, the strength of H_s has been demonstrated. Extracting J_{IC} for that system from pulsed-field data close to a value from previous INS study we confirm the validity of the adopted spin Hamiltonian and the applicability of the SWT. To extract J_{IC} an H_s-study is preferable over INS, due to smaller error bars, the possibility to work with small single crystals and a much higher efficiency (concerning both time and costs). The large H_s obtained from several independent theoretical and experimental studies discards any 1D scenario for Li_2CuO_2, even more, H_s itself is (within the isotropic model) independent of the in-chain couplings J_1 and J_2. Thus, our results show *exactly* that for a rather wide interval $0 < \alpha < 1$ and collinear magnetic order at $H = 0$, H_s depends only on the IC, irrespective of its strength. A complete study of the entire phase diagram including the INC2 phase will be given elsewhere. The MP-phases from 1D studies are very sensitive to the presence of IC in the 2D or 3D systems. In particular, they can be eliminated by a weak AFM IC. Instead new incommensurate phases may occur. A study of H_s in other systems within the approach proposed here is in progress.

We thank the DFG (grants DR269/3-1, KL1824/2, RI615/16-1), PICS program (Contract No. CNRS 4767, NASU 267), EuroMagNET, & EU (Contract No. 228043) for support.

*Corresponding author.
s.l.drechsler@ifw-dresden.de

[1] A. W. Sandvik, Phys. Rev. Lett. **83**, 3069 (1999).
[2] S. Todo *et al.*, Phys. Rev. B **78**, 224411 (2008).
[3] W. E. A. Lorenz *et al.*, Europhys. Lett. **88**, 37002 (2009).
[4] C. Yasuda *et al.*, Phys. Rev. Lett. **94**, 217201 (2005).
[5] S.-L. Drechsler *et al.*, J. Magn. Magn. Mater. **316**, 306 (2007).
[6] A. V. Chubukov, Phys. Rev. B **44**, 4693 (1991).
[7] T. Vekua *et al.*, *ibid.* **76**, 174420 (2007).
[8] F. Heidrich-Meisner *et al.*, *ibid.* **74**, 020403R (2006).
[9] R. O. Kuzian and S.-L. Drechsler, *ibid.* **75**, 024401 (2007).
[10] M. Härtel *et al.*, *ibid.* **78**, 174412 (2008).
[11] D. Dmitriev and V. Krivnov, *ibid.* **79**, 054421 (2009).
[12] L. Kecke *et al.*, *ibid.* **76**, 060407 (2007).
[13] T. Hikihara *et al.*, *ibid.* **78**, 144404 (2008).
[14] J. Sudan *et al.*, *ibid.* **80**, 140402(R) (2009).
[15] R. Zinke *et al.*, *ibid.* **79**, 094425 (2009).
[16] H. T. Ueda and K. Totsuka, *ibid.* **80**, 014417 (2009).
[17] M. Zhitomirsky *et al.*, Europhys. Lett. **92**, 37001 (2010).
[18] L. E. Svistov *et al.*, Pis'ma Zh. Eksp. Teor. Fiz. **93**, 24 (2011) [JETP Lett. **93**, 21 (2011)].
[19] S. R. White, Phys. Rev. Lett. **69**, 2863 (1992).
[20] S. Qin *et al.*, Phys. Rev. B **52**, R5475 (1995).
[21] See Supplemental Material at http://link.aps.org/supplemental/10.1103/PhysRevLett.107.097201 for the phase diagram in terms of α and β_2, details of the calculations, and some thermodynamic constraints.
[22] Its account is possible but electronic structure calculations suggest $J'_{IC}/J_{IC} \leq 0.1$, only.
[23] From the error bars of J_1 and α: ± 5 K and ± 0.005, respectively, we have $7.18\ \text{K} \leq J_{IC}^{cr,+} \leq 8.54$ K, and $J_{IC}^{cr,+}$ is well below the J_{IC} values obtained from the INS or H_s data.
[24] K. Kudo *et al.*, Phys. Rev. B **71**, 104413 (2005).
[25] M. Matsuda *et al.*, *ibid.* **63**, 180403 (2001).
[26] S. Kawamata *et al.*, J. Magn. Magn. Mater. **272–276**, 939 (2004).